Central European Journal of Energetic Materials
ISSN 1733-7178; e-ISSN 2353-1843

Cent. Eur. J. Energ. Mater. 2017, *14*(1): 134-151; DOI: 10.22211/cejem/67678

Coating of $LiBH_4$ and Its Effect on the Decomposition of RDX and AP

Xiaoyong Ding,[1,2] Yuanjie Shu,[1,2*] Zhiqun Chen,[2,3] Ning Liu,[2,3] Bingwang Gou,[2,3] Jianguo Zhang,[1] Minjie Wu,[2,3] Gang Xie,[4] Taotao Dang[4]

[1] *State Key Laboratory of Explosion Science and Technology, Beijing Institute of Technology, Beijing 100081, China*
[2] *State Key Laboratory of Fluorine & Nitrogen Chemicals, Xi'an, Shaanxi 710065, China*
[3] *Xi'an Modern Chemistry Research Institute, Xi'an, Shaanxi 710065, China*
[4] *School of Chemical Engineering and Material, Northwestern University, Xi'an, Shaanxi 710069, China*
[*] *E-mail: 1204172675@qq.com*

Abstract: The novel fuel additive $LiBH_4$ was introduced as an energetic component for its outstanding hydrogen content, perfect burning performance and high reactivity. In order to limit the hygroscopicity and to improve the stability in the air, $LiBH_4$ was coated on the surface with wax and polyester carbonate. The final product was characterized by scanning electron microscopy (SEM), X-ray photoelectron energy spectroscopy (XPS) and Raman spectroscopy, while the stability in air was investigated by regular checking of variations in weight. The results show that a uniform coating layer was formed on the surface of the $LiBH_4$, and the coverage was estimated from the boron content as approximately 82%. A healing effect was confirmed on defective surfaces exposed to air; the coating layer improves the relative stability by 50.7%. Furthermore, $LiBH_4$ as an additive to promote the thermal decomposition of 1,3,5-trinitro-1,3,5-trazinane (RDX) and ammonium perchlorate (AP) was explored by differential scanning calorimetry (DSC), in which the catalytic effects of pure $LiBH_4$ and coated $LiBH_4$ were compared, and indicated that the coating does not decrease the reactivity of $LiBH_4$. It is suggested that surface coating with some inert materials is a simple and effective method for improving the storage and performance of $LiBH_4$, while ensuring its reactivity.

Keywords: coating, hydride, additive, hygroscopicity, DSC

1 Introduction

Recently, metal hydrides have received extensive attention not only as hydrogen storage materials but also as additives in energetic materials, owing to their outstanding properties in the processes of combustion and explosion [1-5]. As a particularly high hydrogen content contributes to the wide application for energy storage carriers, metal hydrides similarly benefit combustion in propellants by releasing molecular H_2 and intensifying the explosion through the strong exothermic reaction. As a matter of fact, metal hydrides were suggested as energetic additives decades ago. In the early 1960s, Joseph [6] conducted research on the energetic performance of organic energetic materials with magnesium hydride. For TNT, tetryl, C-4 and other explosives, a remarkable explosion enhancing capacity was observed for explosives containing MgH_2. Chinese scientists focused mainly on lithium hydride and deuteride for nuclear weapons [7, 8]. Recently, Cheng *et al.* [9] investigated the detonation characteristics of modified emulsion explosives by introducing TiH_2 and MgH_2. It was found that these hydrogen storage materials provided good improvement in the explosion power while remarkably increasing the decay time and shock wave overpressure by 42% and 32%, respectively. Instead of aluminum, AlH_3 was introduced by Yao *et al.* [10] in solid propellants and the impulse could be enhanced by over 100 $N \cdot s \cdot kg^{-1}$. In these researches, metal hydrides were suggested to be preferable additives in special blasting operations.

$LiBH_4$ is an outstanding complex metal hydride among the chemical hydrides, with the largest hydrogen gravimetric density of up to 18.5% and a very high volumetric hydrogen density (121 $kg \cdot m^{-3}$) [11]. These provide $LiBH_4$ with great potential as an additive in energetic materials. However, $LiBH_4$ and other alkali metal compounds suffer from unfavorable chemical stability and are regarded as hazardous materials [12-15]. That is why $LiBH_4$ mostly appears in theoretical studies, and is rarely found in industrial use [16-18]. To inhibit the hygroscopicity of materials, purification [19], spheroidizing [20] and surface coating [21] have been proposed as common measures. In consideration of the environmental sensitivity, there is a high risk from the former two methods. Jenkin [22] introduced pyrolysis metal compounds and designed complex equipment for complex encapsulation of $LiBH_4$ as a new method. However, he did not demonstrate a specific encapsulating effect. In addition, high temperature and a corrosion resistant environment, expensive investment and uncertain safety limit the feasibility.

In the present study, we conducted a beneficial trial for coating $LiBH_4$ with inert materials of alkanes and carbonic ester structures. Scanning electron microscopy (SEM), X-ray photoelectron energy spectroscopy (XPS) and Raman

spectroscopy were applied to estimate the coating efficiency, while the stability in air was investigated by regular study of variations in weight. In addition, the catalytic effect of $LiBH_4$ on the thermal behaviour of 1,3,5-trinitro-1,3,5-trazinane (RDX) and ammonium perchlorate (AP) were explored, mainly by differential scanning calorimetry (DSC).

2 Experimental

2.1 Materials and preparation

The $LiBH_4$ powder used in these experiments was purchased from Alfa Aesar Company (St. Paul, MN, USA). The purity was 95%, with average particle size 10-20 μm. The inert materials used included the traditional coating material paraffin wax [23] and waterproof material polyester carbonate [24]. The paraffin wax (m.p. 68.15 °C) and polyester carbonate (abbreviated as PC, m.p. 260 °C) were purchased from Chinese Petrochemical Joint Stock Limited Company and Dongguan Lixin Plastic Limited Company respectively. Paraffin wax and PC were dissolved in appropriate solvents and mixed, $LiBH_4$ being then added to form a homogeneous mixture [25]. After the solvents had been evaporated under vacuum, the coated $LiBH_4$ was obtained as a dry powder. In this coating process, the total mass of wax and PC was 5%.

1,3,5-Trinitro-1,3,5-trazinane and ammonium perchlorate were representative energetic materials and were synthesized by Xi'an Modern Chemistry Institute, with powder size 10-50 microns. Mixtures of RDX (or AP) and $LiBH_4$ powders were prepared by grinding the two components in a polished carnelian mortar for 1 h.

2.2 Scanning electron microscopy

The morphology and particle size of pure $LiBH_4$ and coated $LiBH_4$ were investigated using a field emission scanning electron microscope (FE-SEM; Hitachi JEOL-6301, Hitachi, Japan).

2.3 X-ray photoelectron spectroscopy

Surface chemical analysis was determined by X-ray photoelectron spectroscopy (XPS) on C1s, O1s, B1s and Li1s elements, scanning with an Al Kα radiation source. The voltage, current and vacuum degree applied were 12 kV, 6×10^{-3} A and 1.067×10^{-5} Pa, respectively. The test was carried out on a circular area, radius 400 μm, on samples, the test depth was 5-10 nm. The peak of C1s at 284.39 eV was used as the reference. The XPS apparatus used was made by Aoke.

2.4 Raman spectroscopy

Raman spectroscopy was implemented with a Renishaw inVia Raman instrument, and the excitation source was a 785 nm laser with power about 250 mW. Experiments were carried out at room temperature.

2.5 Measuring balance

A precise balance (0.1 mg precision) by Mettler Toledo Company was used in the further mass variation experiments in order to investigate the environmental stability. Pure $LiBH_4$ and coated $LiBH_4$ samples (0.03 g) were weighed and recorded every 30 min for 4 h in a normal atmosphere, when the temperature was 25 °C and the humidity was 55%.

2.6 Differential scanning calorimetry

Differential scanning calorimetry is a routine technique to study thermal stability, heat generation, kinetic parameters, decomposition of reactive substances, *etc*. In this research, the DSC apparatus used was made by Netzsch (type: DSC404 F3). The sample was placed in an alumina crucible with a hole in the lid and heated in a high purity nitrogen atmosphere at a heating rate of 10 °C/min from 25 °C to 500 °C. A stainless steel crucible was also used.

2.7 Powder X-ray diffraction

X-ray diffraction (XRD) was utilized to analyze the phase components of the samples. The XRD apparatus used was made by Bruker (type: D8 ADVANCE, Cu Kα radiation source).

3 Results and Discussion

3.1 Characterization of $LiBH_4$

3.1.1 SEM analysis

Figure 1 shows SEM images of pure $LiBH_4$ and coated $LiBH_4$ morphology. The original $LiBH_4$ particles are angular, with a rough surface. $LiBH_4$ shows a relatively fine uniformity of particle size. Due to the significant expandability of warm paraffin wax and PC, compact and smooth surfaces were observed after coating.

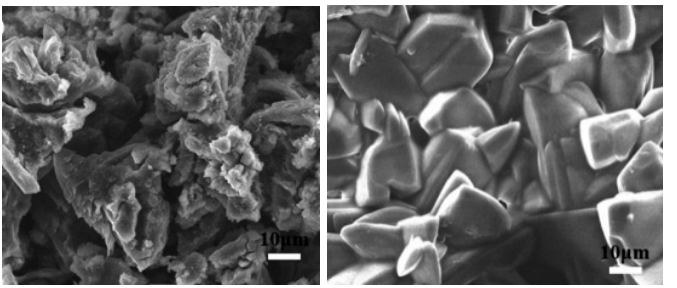

Figure 1. SEM images of pure $LiBH_4$ and coated $LiBH_4$

3.1.2 XPS analysis

XPS technology was used to test the elemental content on the surface of coated $LiBH_4$. The atomic mass fraction of elements was obtained as shown in Table 1.

The coating materials were composed of the elements hydrogen, oxygen and carbon. However, hydrogen is barely observed in photoelectron spectroscopy, while the actual amounts of oxygen and carbon atoms are often disturbed by a variety of factors. Therefore, boron was generally chosen as appropriate to calculate the relative contents and to estimate the coating efficiency. If coated completely, there would be no boron on the surface. As shown in Table 1, boron is still observed on the coated surface, indicating that the coating is less than 100%. Through the above analysis, the boron atomic mass fraction on the surface was used to estimate the relative coating, which was calculated using Formula 1:

$$B(1-R_C)=B' \tag{1}$$

where, R_C is the relative coating; B is the mass fraction (boron) on the surface of the $LiBH_4$; B' is the mass fraction (boron) on the surface of the coated $LiBH_4$.

Table 1. XPS test results of coated $LiBH_4$

Content	B	C	O	Li	Others	R_C/100%
Pure [wt.%]	64.31	-	-	35.58	0.11	0
Coated [wt.%]	11.48	57.22	27.42	6.09	0.12	82

R_C reflects the relative change of mass fraction (boron) on the sample surface under different conditions. The greater its value is, the more complete is the coating [26]. R_C was 82% in the XPS test, indicating that the coating material was wrapped over the surface of the $LiBH_4$ in a uniform thin film layer.

3.1.3 Raman analysis

It was shown to be difficult for a powder of a large specific surface area to be completely coated according to the coating efficiency calculated above. The uncoated surface defects provided a reaction path for $LiBH_4$ in air. In this process, reaction between $LiBH_4$ and H_2O existed, resulting in the release of hydrogen and the generation of lithium boron oxide.

The Raman peak intensities were measured on pure $LiBH_4$ and coated $LiBH_4$ by an in-situ micro Raman spectrometer, and the results are shown in Figure 2.

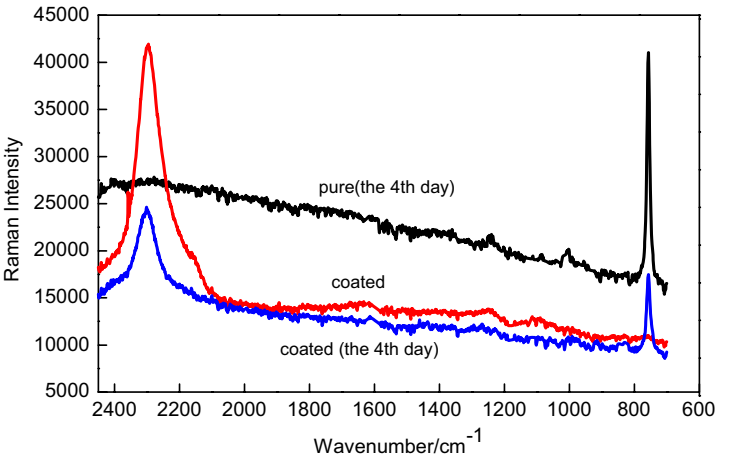

Figure 2. Raman intensities of samples

As shown in Figure 2, the Raman peak around 2300 cm^{-1} corresponds to the stretching vibration of BH_4^- [27, 28], and the peak at 757 cm^{-1} is the vibration of the degradation products. The corresponding B−H spectral peaks are still observed for coated $LiBH_4$ after 4 days in air, while the spectral peaks for pure $LiBH_4$ disappeared completely.

3.1.4 Quantitative analysis

The hydrolysis reaction of $LiBH_4$ under normal pressure and temperature was carried out on a bed of powder. The mass variation of the sample was recorded by a precise balance and typical mass increases for the material are presented in Figure 3.

Due to the light quality of the $LiBH_4$, hydrolysis in the atmosphere produced a significant increase in weight, which was used to characterize the stability in air. Figure 3 (a) is the mass change of the samples during the time exposed in air, and the initial mass state is 0; Figure 3 (b) is the mass of the remaining $LiBH_4$

calculated from Formula 2, the initial value is 1.

$$LiBH_4(s) + 4H_2O(g) \rightarrow LiBO_2 \cdot 2H_2O(s) + 4H_2(g) \quad (2)$$

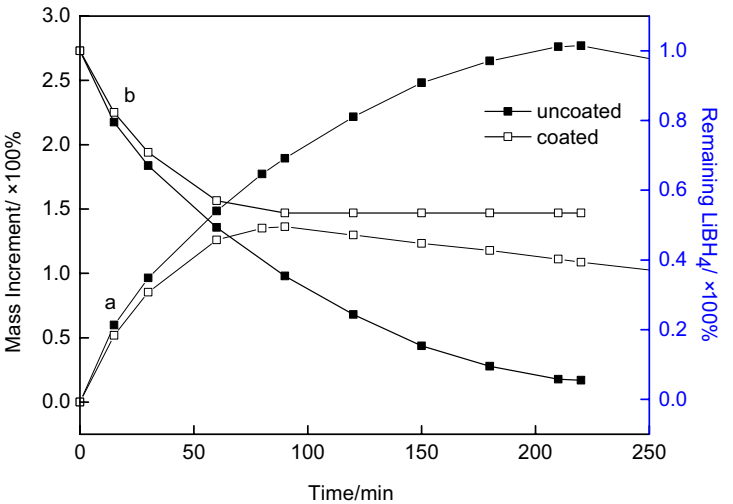

Figure 3. Mass increments of sample − a; Remaining $LiBH_4$ mass − b

As shown in Figure 3 (a), the masses of both samples experience an initial increase and then a decrease with time. The first process is moisture absorption on the exposed surface of the $LiBH_4$. After a few minutes of exposure, dissolution of pure $LiBH_4$ in H_2O occurred and vigorous bubbling was observed. Hydrogen loss was lighter than oxygen absorbed, thus the initial reaction maintained a high mass increase rate. After the rapid mass gained by hydrolysis within 1 h, the remaining $LiBH_4$ was 48% of the initial mass, and the average mass increase rate was 0.0159 g/h; only 24% was left after 2 h in air, during which period the average mass increase rate was 0.0114 g/h. Coated $LiBH_4$ experienced a mass increase within 1 h, with an average mass increase rate of 0.0126 g/h, and left 57% of the initial mass intact in the experiment.

During the hydrolysis process, solid product gradually condensed on the bare surface of the $LiBH_4$, which prevented the entry of air and decreased the hydrolysis rate. However, uncoated $LiBH_4$ exposed a broad reaction area on its surface, so that a fast and lasting reaction existed until substantially complete reaction of the $LiBH_4$. By contrast, the remaining mass of coated $LiBH_4$ was maintained at 53%.

After complete hydrolysis of $LiBH_4$, according to the reaction Formula 2 [12], the condensed product will have increased up to 2.93 times in mass. The subsequent mass loss is ascribed to the dehydration process. In these experiments,

the maximum mass of the product reached 2.76 times that of the pure $LiBH_4$ before hydrolysis, and the reaction extent was 94.2%. As for the coated sample, the highest mass gain was only 1.36 times, and the reaction extent was 46.4%. The stability was increased 50.7%, as estimated from the reacted $LiBH_4$ mass, which indicates that the coating layer effectively improves the stability of the $LiBH_4$.

3.2 Effect on representative energetic materials

In order to explore $LiBH_4$ as an additive in mixed explosives, its effect on the thermal decomposition of RDX and AP was studied. All samples were handled in small quantities (within 1 mg) and ground gently to obtain an even distribution. Moreover, the appropriate safety precautions were taken.

3.2.1 Thermal behaviour of $LiBH_4$ powder

The DSC decomposition curve of pure $LiBH_4$ is shown in Figure 4. Two endothermic peaks and one exothermic peak were observed. In the first stage, a polymorphic transformation occurs around 115.7 °C and a small amount of decomposition occurs. Bulk decomposition commences near the melting point (MP) of $LiBH_4$ (285.2 °C, 1 bar). Subsequent continuous dehydrogenation reactions occur from about 300 °C. The base lines were well calibrated, but the DSC curves of $LiBH_4$ drifted badly downwards in repeated experiments. The phenomenon was similar to that in previous researches [29, 30], and may be attributed to the continuous hydrolysis reaction of $LiBH_4$. Further reasons for this behavior may be related to the particle size and other uncertain factors.

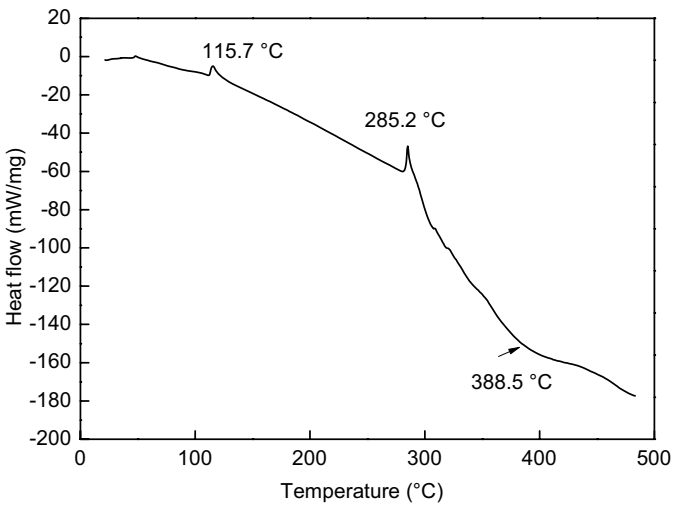

Figure 4. DSC curve of $LiBH_4$

3.2.2 RDX and RDX/LiBH₄

A sample of RDX/$LiBH_4$ was ground dry and mixed in an agate crucible. The $LiBH_4$ here experienced no coating process. Amounts (0.6 mg) of RDX/$LiBH_4$ were tested in different mass ratios of 100/0, 95/5, 90/10 and 50/50 respectively. Figure 5 shows the DSC curves of RDX and the mixtures of RDX and $LiBH_4$. More details are given in Table 2.

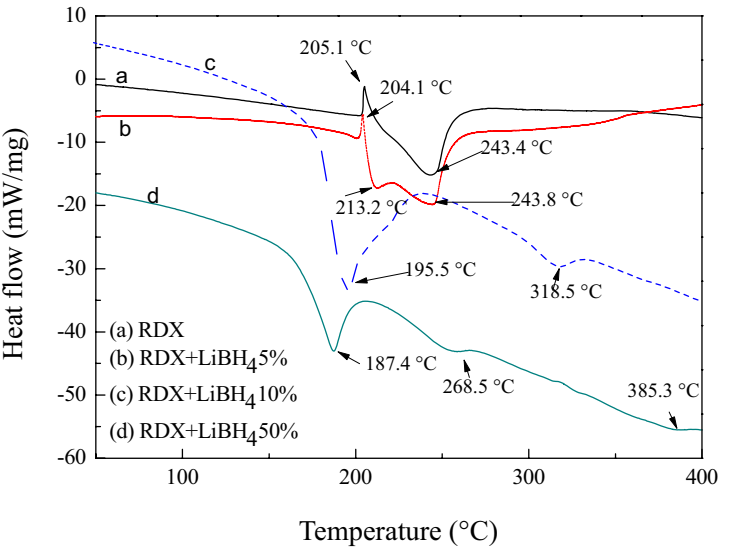

Figure 5. DSC curve of RDX/$LiBH_4$ mixtures

Table 2. Data from DSC analyses on RDX and RDX/$LiBH_4$ mixtures

Sample	m [mg]	T_M [°C]	Decomposition process			
			T_{p1} [°C]	T_{p2} [°C]	T_{p3} [°C]	ΔH_d [J·g^{-1}]
RDX	0.6	205.1	-	243.4	-	1137.7
RDX/$LiBH_4$ 5%	0.6	204.1	213.2	243.8	-	2031.3
RDX/$LiBH_4$ 10%	0.6	-	195.5	-	318.5	3651.4
RDX/$LiBH_4$ 50%	0.6	-	187.4	268.5	385.3	991.5

The obvious peaks of pure RDX at 205.1 °C and 243.4 °C signify a melting endothermic process and decomposition into volatile products [31, 32]. As for the thermal decomposition mechanism of RDX, Brill and Brush [33] investigated this and proposed that C–N and N–N bonds break simultaneously, as shown in Formulas 3 and 4:

$$(CH_2NNO_2)_3 \rightarrow 3\ (CH_2O + N_2O) \quad (3)$$

$$(CH_2NNO_2)_3 \rightarrow 3\ (HCN + H\cdot + NO_2) \quad (4)$$

When 5% $LiBH_4$ was added to RDX, two exothermic peaks appeared in the curve and a similar phase transition almost identical with pure RDX. As shown in Figure 4, the main decomposition temperature of $LiBH_4$ is above 300 °C. The new exothermic peak at 213.2 °C may be assigned to a competition between Formulas 3 and 4 [33]. The cleavage of C–N bonds is the dominant reaction and causes a gentle and slow heat release in the early stages of decomposition. Palopoli and Brill [34] pointed out that cleavage of the N–N bonds of cyclic nitramines may be attributed to its alkyl H atoms transferring to nearby $–NO_2$ groups. Therefore, the bond breaking reaction benefits from H atoms in $LiBH_4$ transferring to the $–NO_2$ groups, together with those in the $–CH_2–$ groups. More oxidizer, NO_2, is generated and reacts with $LiBH_4$ and its degradation products and provides extra heat before being removed by the N_2 gaseous flow [35].

Based on the above analysis, the melting peak disappeared when $LiBH_4$ was added in 10% and 50% amounts, and the large exothermic peaks of RDX appeared instead. It is obvious that RDX tends to a direct decomposition without melting in the presence of enough $LiBH_4$. The peak temperatures of RDX/$LiBH_4$ at different mass ratios were much lower than that of pure RDX, and decreased by 47.9 °C (10% $LiBH_4$) and 56 °C (50% $LiBH_4$) respectively. This indicates that $LiBH_4$ acts as a catalyst in the decomposition of RDX-based explosives. When $LiBH_4$ was added from zero to 10%, an obvious linear increase in heat released by RDX decomposition was observed. As Table 2 shows, the exothermic heat quantity from RDX had increased by 78.5% (5% $LiBH_4$), and 220.9% (10% $LiBH_4$), respectively. However, when $LiBH_4$ was added at 50% by mass, the content of the main explosive RDX was immediately decreased and also the heat released. Although a lower decomposition temperature of RDX was observed, there was a lot of $LiBH_4$ residue, as the small but obvious peaks on the DSC curves of RDX/$LiBH_4$ (10% and 50%) indicate. These introduced peaks are recognized respectively as dehydrogenation reactions (318.5 °C and 385.3 °C) and the melting point (268.5 °C) of $LiBH_4$ [36-38]. As a result, there should exist a best mass ratio region in the different mixture systems, an optimum value for generating the highest temperature decrease and process heat at the same time.

As for the catalytic mechanism, it can be inferred that there are two reaction stages between $LiBH_4$ and RDX. The released hydrogen participates in the decomposition of RDX first and degradation products from both RDX and $LiBH_4$ react with each other in the following stage. Xue *et al.* [39] found that

decomposition and oxidation reactions coexist for metal hydrides in his explosion experiments on the RDX/TiH_2 system.

It is known [40] that small quantities of Al particles prove to be inert materials which hinder the thermal decomposition of energetic materials. Only when the Al content is more than 40% mass do the Al particles play a catalytic role. In this respect, $LiBH_4$ is evidently superior to Al particles. A greater $LiBH_4$ content leads to an easier thermal explosion and a higher thermal sensitivity within a certain range. The addition of $LiBH_4$ to explosives may help to increase the reaction duration of the explosion and to improve the detonation power.

For samples containing coated $LiBH_4$, the decomposition of RDX shifted to lower temperatures (shown in Table 3) than those for mixtures containing an equivalent amount of pure $LiBH_4$ (shown in Table 2). In addition, the heat released is increased. However, the melting peak of RDX for RDX/coated $LiBH_4$ (10%) is relatively clear, indicating that the opportunity for reaction between $LiBH_4$ and RDX is reduced to some extent by the coating layer. The obvious peaks for $LiBH_4$ were also lowered. Generally, the catalytic effect of coated $LiBH_4$ was more remarkable.

Table 3. Data from DSC analyses on RDX and RDX/coated $LiBH_4$ mixtures

Sample	m [mg]	T_M [°C]	Decomposition process			
			T_{p1} [°C]	T_{p2} [°C]	T_{p3} [°C]	ΔH_d [J·g^{-1}]
RDX	0.6	205.1	-	243.4	-	1137.7
RDX/$LiBH_4$ 5%	0.6	203.0	-	236.9	-	3825.1
RDX/$LiBH_4$ 10%	0.6	203.2	208.9	-	314.3	1103.6
RDX/$LiBH_4$ 50%	0.6	-	161.6	257.0	372.3	1022.4

XRD and XPS measurements were performed on RDX/coated $LiBH_4$ (50%) to obtain more information about the reaction. The XRD patterns of $LiBH_4$ in the samples before and after the DSC test are shown in Figure 6. LiOH was also detected besides $LiBH_4$ in the powder, as shown in Figure 6 (a). After the DSC analysis, the solid powder was recognized as Li_2CO_3, while the B and H elements were mainly released as gaseous products. B_2H_6 was believed to be a possible product [30], and may react with N_2 to form BN, as was shown in Figure 6 (b).

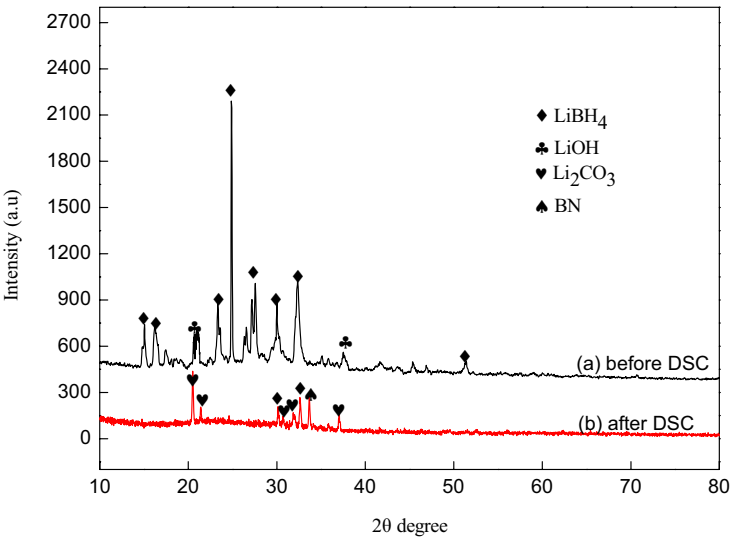

Figure 6. XRD patterns of $LiBH_4$ from RDX/$LiBH_4$ (50%)

The XPS results on the reaction products show that the major elements are O, C, B and Li (Table 4). A comparison of our XPS results with standard XPS spectra allowed us to identify Li_2CO_3 and BN at 55.3 eV and 190.8 eV, respectively. This is consistent with the results in the XRD test for powder product analysis in Figure 6.

Table 4. XPS data for elements in the reaction products after DSC

Element	Binding energy [eV]
Li 1s	55.3
B 1s	190.8
C 1s	284.39
O 1s	531.89

Combined with the analysis of the reaction products, we consider that for the metal Li^+ part, the formation of metal oxides on the surface of the energetic materials could contribute to a further catalytic effect. For the BH_4^- part, this has a more important effect on increasing the heat generated during thermal decomposition and possibly burning at high temperature. The possible overall reaction between RDX and $LiBH_4$ can be expressed as Formula 5.

$$2LiBH_4 + C_3H_6N_6O_6 = Li_2CO_3 + BN + 0.5B_2H_6 + 2CO + H_2O + 2.5N_2 + 4.5H_2 \quad (5)$$

3.2.2 AP and AP/LiBH₄

As the most common oxidizer used in propellants, explosives and pyrotechnics, AP has attracted considerable research on its thermal decomposition [41]. Our research on AP/$LiBH_4$ was conducted under the same conditions as RDX/$LiBH_4$. Figure 7 shows the DSC curves of AP/$LiBH_4$ and mixtures of AP with coated $LiBH_4$.

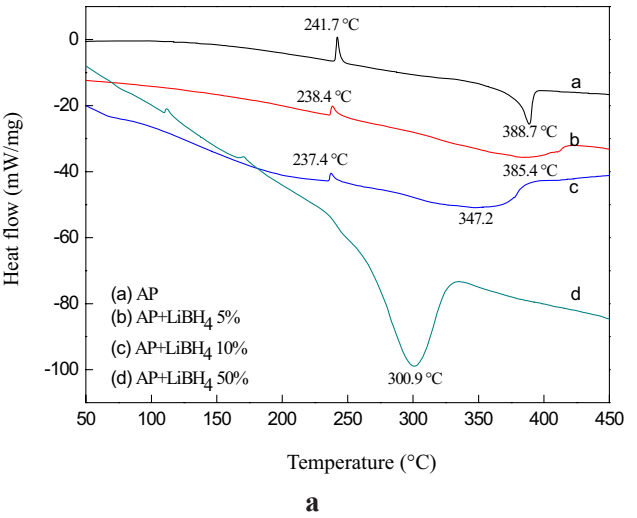

a

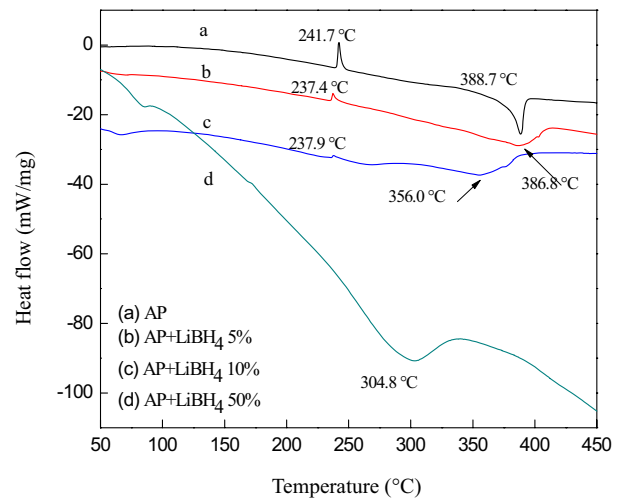

b

Figure 7: a. DSC curves of AP/$LiBH_4$ and **b.** AP/coated $LiBH_4$

Table 5. Data from DSC analyses on AP and AP/$LiBH_4$ mixtures

Sample	m [mg]	T_M [°C]	Decomposition process	
			T_p [°C]	ΔH_d [J·g^{-1}]
AP	0.6	241.7	388.7	792
AP/$LiBH_4$ 5%	0.6	238.4	385.4	1041
AP/$LiBH_4$ 10%	0.6	237.4	347.2	1083
AP/$LiBH_4$ 50%	0.6	-	300.9	3503
coated $LiBH_4$ 5%	0.6	237.4	386.8	945.6
coated $LiBH_4$ 10%	0.6	237.9	356.0	996
coated $LiBH_4$ 50%	0.6	-	304.8	1608

Figure 7 shows the DSC curves of the mixtures of AP with $LiBH_4$ and coated $LiBH_4$. The endothermic peak of AP in Figure 7 at 241.7 °C corresponds to its crystal transformation from orthorhombic to the cubic phase [42]. The exothermic peak at 388.7 °C is attributed to the decomposition of AP [43, 44]. From Figure 7, it is observed that pure $LiBH_4$ (no higher than 10% in mass fraction) had no significant impact on the phase transition position. However it did influence the decomposition patterns of AP. The sharp exothermic peak became moderated when $LiBH_4$ was added, which indicates a prolonged decomposition process.

The exothermic peak in pure AP had moved from 388.7 °C to 385.4 °C for AP/$LiBH_4$ (5%) and was broader in the presence of $LiBH_4$. It is apparent that the exothermic peak temperature of AP/$LiBH_4$ (10%) and AP/$LiBH_4$ (50%) was much lower than that of pure AP (388.7 °C); it had decreased by 41.5 °C and 87.8 °C, respectively. Because the decomposition temperature of AP is much higher than that of RDX and closer to that of $LiBH_4$, the exothermic peaks may be mixed peaks of both AP and $LiBH_4$, and the decomposition process is prolonged. No obvious peaks appeared for $LiBH_4$. The heat released for the sample containing 50% $LiBH_4$ was far greater than for the other samples, confirming the analysis. Control experiments were performed in which coated $LiBH_4$ was introduced, and the results were similar to those with pure $LiBH_4$. Although the temperature of the exothermic peak decreased a little (1.4-8.8 °C) compared with pure $LiBH_4$, the thermal activity of coated $LiBH_4$ was still maintained and was not affected much by the inert material.

In conclusion, both $LiBH_4$ and coated $LiBH_4$ show good catalytic effects on the thermal decomposition of RDX and AP. The highest decrease in values for the mixed systems of RDX/$LiBH_4$ and AP/$LiBH_4$ were 56 °C and 87.8 °C, respectively. It may be inferred that in the mixed systems of RDX/$LiBH_4$ and AP/$LiBH_4$, the compounds decompose and release much heat individually, which enhances the total heat processes of the mixtures. In terms of a catalytic

mechanism, we consider that the formation of metal oxides at the molecular level on the surface of an energetic material could enhance their effect further.

4 Conclusions

(1) A simple coating method was proposed and used for a light metal hydride powder, and a thin uniform film layer comprised of inert material was formed on the $LiBH_4$ surface; the relative coverage of $LiBH_4$ was 82%.
(2) Thermal analysis revealed that the protective covering layer can improve the stability of $LiBH_4$ in air for a relatively long time while uncoated $LiBH_4$ reacts quickly in air and becomes exhausted. Hydrolysis products slightly formed on covering film defects, contributing to preventing further reaction of $LiBH_4$ exposed in the normal atmosphere. 53% of the $LiBH_4$ sample was effectively sealed by the covering film, and its stability was increased by 50.7%.
(3) DSC experiments revealed that both pure and coated $LiBH_4$ showed prominent effects on the thermal decomposition of RDX and AP. The decomposition of RDX and AP was accelerated. The coating does not reduce the activity of $LiBH_4$.

Acknowledgements
This work was supported by a grant from the National Natural Science Foundation of China (Grant No. 51373159), and the International Cooperation and Exchange of the National Natural Science Foundation of China (Grant No. 51511130036).

References

[1] Xi, J.F.; Liu, J.Z.; Wang, Y.; Liang, D.L.; Zhou, J.H. Effect of Metal Hydrides on the Burning Characteristics of Boron. *Thermochim. Acta* **2004**, *597*: 58-64.
[2] Sakintuna, B.; Lamari-Darkrim, F.; Hirscher, M. Metal Hydride Materials for Solid Hydrogen Storage: a Review. *Int. J. Hydrogen Energy* **2007**, *32*: 1121-1140.
[3] Graetz, J.; Reilly, J. J. Thermodynamics of the α, β and γ Polymorphs of AlH_3. *J. Alloys Compounds* **2006**, *424*: 262-265.
[4] Ren, R.M.; Ortiz, A.L.; Markmaitree, T.; Osborn, W.; Shaw, L.L. Stability of Lithium Hydride in Argon and Air. *J. Phys. Chem. B* **2006**, *110*: 10567-10575.
[5] Pitt, M.P.; Paskevicius, M.; Brown, D.H.; Sheppard, D.A.; Buckley, C.E. Thermal Stability of $Li_2B_{12}H_{12}$ and its Role in the Decomposition of $LiBH_4$. *J. Am. Chem. Soc.* **2013**, *135*(18): 6930-6941.

[6] Joseph, R.H. *Enhanced Organic Explosives*. Patent US 3012868, **1961**.
[7] Xiong, H.L.; Chen, X.P. Determination of Variation Mathematic Model of Tritium in Lithium Deuteride-Tritide. *Aviation Metrology & Measurement Technology* **1999**, *19*(5): 1-7. (in Chinese)
[8] Ma, Y.M.; Cui, T.; He, W.J.; Zhou, Q.; Liu, Z.M.; Zou, G.T. Pressure and Temperature Effects on the System of Lithium Doped in Solid D_2. *Chinese J. High Pressure Phys*. **2003**, *17*(2): 88-94.
[9] Cheng, Y.F.; Ma, H.H.; Liu, R.; Shen, Z.W. Explosion Power and Pressure Desensitization Resisting Property of Emulsion Explosives Sensitized by MgH_2. *J. Energ. Mater*. **2014**, *32*(3): 207-218.
[10] Yao, X.L.; Cao, Y.L.; He, J.X. Aluminum Hydride − High Energy Fuel of Solid Propellant. *Chinese J. Energ. Mater.* **2014**, *12*(z1): 161-165. (in Chinese)
[11] Zŭttel, A. Materials for Hydrogen Storage. *Mater Today* **2003**, *6*(9): 24-33.
[12] Goudon, J.P.; Bernard, F.; Renouard, J.; Yvart, P. Experimental Investigation on Lithium Borohydride Hydrolysis. *Int. J. Hydrogen Energy* **2010**, *35*(20): 11071-11076.
[13] Murtomaa, M.; Laine, E.; Salonen, J.; Kuusinen, O. On Effects of Ambient Humidity on Sodium Borohydride Powder. *Powder Handling Process* **1999**, *11*: 87-90.
[14] Haertling, C.; Hanrahan, R.J.; Smith, R. A Literature Review of Reactions and Kinetics of Lithium Hydride Hydrolysis. *J. Nucl. Mater*. **2006**, *349*: 195-233.
[15] Li, C.; Peng, P.; Zhou, D.W.; Wan, L. Research Progress in $LiBH_4$ for Hydrogen Storage: a Review. *J. Hydrogen Energy* **2011**, *36*: 14512-14526.
[16] Li, C.; Zhou, D.W.; Peng, P.; Wan, L. First-principles Calculation on Dehydrogenating Properties of $LiBH_4$-X (X=O, F, Cl) Systems. *Acta Chim. Sin.* **2012**, *70*(1): 71-77.
[17] Schlapbach, L.; Zŭttel, A. Hydrogen Storage Materials for Mobile Application. *Nature* **2001**, *414*: 353-358.
[18] Lei, H. J.; Duan, H.; Xing, P. F.; Tang, Y. J. Synthesis and Application of ADN Oxidizer. *Aerosol Sci. Technol*. **2011**, *10*: 1165-1169.
[19] Steinbach, T.; Wahlen, C.; Wurm, F.R.; Poly (Phosphonate)-mediated Horner-Wadsworth-Emmons Reactions. *Polymer Chemistry* **2015**, *6*(7): 1192-1202.
[20] He, L.M.; Xiao, Z.L.; Jing, D.Q.; Dong, F.Y. Synthesis and Application of ADN Oxidizer in Propellant. *Chinese J. Energ. Mater*. **2003**, *11*(3): 170-173. (in Chinese)
[21] Cui, Q.Z.; Jiao, Q.J.; Ren, H.; Yang, R.J. Study on Moisture-resistant Black Powder. *Chinese J. Energ. Mater*. **2007**, *15*(2): 114-117. (in Chinese)
[22] Jenkin, W.C. *Method of Encapsulation of Lithium Borohydride*. Patent US 3070469, **1962**.
[23] Nan, H.; Guo, X.; Sun, P.P.; Niu, Y.L.; Tian, X. The Influence of Coating Material on the Impact Sensitivity of AP Powder. *Initiators & Pyrotechnics* **2013**, *6*: 39-41.
[24] Jiang, B.B. Preparation of Core-shell Polycarbonate/BaS04 Submicron Composite Particles. *Chemical Reaction Engineering and Technology* **2005**, *21*(3): 285-288. (in Chinese)
[25] Shu, Y.J.; Ding, X.Y.; Chen, Z.Q.; Wu, M.J.; Liu, N.; Li, Y.N.; Zhai, L.J.; Xu, L.P.

Study on Surface Structural Characterization and Stability of Coated Lithium Borohydride. *Chinese J. Explos. Propellants* **2015**, *38*(2): 30-34. (in Chinese)

[26] Li, J.C.; Jiao, Q.J.; Ren, H.; Wang, L.X.; Zhao, W.D. RDX Coated with Hyantoin/Triazines Composite Bonding Agent. *Chinese J. Energ. Mater.* **2008**, *16*(1): 56-60. (in Chinese)

[27] Gomes, S.; Hagemann, H.; Yvon, K. Lithium Boro-hydride $LiBH_4$: II. Raman Spectroscopy. *J. Alloys Compd.* **2002**, *346*: 206-210.

[28] Racu, A.M.; Schoenes, J.; Lodziana, Z.; Borgschulte, A.; Züttel, A. High-resolution Raman Spectroscopy Study of Phonon Modes in $LiBH_4$ and $LiBD_4$. *J. Phys Chem A*. **2008**, *112*: 9716-9722.

[29] Zhang, Y.; Zhang, W.S.; Wang, A.Q.; Sun, L.X.; Fan, M.Q.; Chu, H.L.; Sun, J.C.; Zhang, T. $LiBH_4$ Nanoparticles Supported by Disordered Mesoporous Carbon: Hydrogen Storage Performances and Destabilization Mechanisms. *J. Hydrogen Energy* **2007**, *32*: 3976-3980.

[30] Zhang, B.J.; Liu, B.H. Hydrogen Desorption from $LiBH_4$ Destabilized by Chlorides of Transition Metal Fe, Co, and Ni. *J. Hydrogen Energy* **2010**, *35*: 7288-7294.

[31] Chen, P.; Zhao, F.Q.; Yin, C.M. Study on Thermal Decomposition Property of RDX/AP/HTPB Propellant. *J. Solid Rocket Technology* **2002**, *25*(2): 52-55. (in Chinese)

[32] Chen, D.; Huang, S.L.; Zhang, Q.; Yu, Q.; Zhou, X.Q.; Li, H.Z.; Li, J.S. Two Nitrogen-rich Ni(II) Coordination Compounds Based on 5,5'-Azotetrazole: Synthesis, Characterization and Effect on Thermal Decomposition for RDX, HMX and AP. *RSC Advances* **2015**, *5*: 32872.

[33] Brill, T.B.; Brush, P.J. Condensed Phase Chemistry of Explosives and Propellants at High Temperature: HMX, RDX and BAMO. *Philos. Trans. R. Soc*. **1992**, *339*: 377-385.

[34] Palopoli, S.F.; Brill, T.B. Thermal Decomposition of Energetic Materials 52. On the Foam Zone and Surface Chemistry of Rapidly Decomposing HMX. *Combust. Flame* **1991**, *87*(1): 45-60.

[35] Bouaricha, S.; Huot, J.; Guay, D.; Schulz, R. Reactivity during Cycling of Nanocrystalline Mg-based Hydrogen Storage Compounds. *Int. J. Hydrogen Energy* **2002**, *27*(9): 909-913.

[36] Soulié, J.Ph.; Renaudin, G.; Cerný, R.; Yvon, K. Lithium Boro-hydride $LiBH_4$: I. Crystal Structure. *J. Alloys Compd*. **2002**, *346*: 200-205.

[37] Hagemann, H.; Gomes, S.; Renaudin, G.; Yvon, K. Raman Studies of Reorientation Motions of $[BH_4]^-$ Anions in Alkali Borohydrides. *J. Alloys. Compd.* **2004**, *363*: 129-132.

[38] Orimo, S.; Nakamori, Y.; Züttel, A. Material Properties of MBH_4 (M =Li, Na, and K). *Mater. Sci. Eng. B*. **2004**, *108*: 51-53.

[39] Xue, B.; Ma, H.H.; Shen, Z.W. Air Explosion Characteristics of a Novel TiH_2/RDX Composite Explosive. *Combust. Explos. Shock Wave (Engl. Transl.)* **2015**, *51*(4): 488-494.

[40] Liu, R.; Yang, L.; Zhou, Z.N.; Zhang, T.L. Thermal Stability and Sensitivity of

RDX-based Aluminized Explosives. *J. Therm. Anal. Calorim*. **2013**; DOI 10.1007/s10973-013-3468-6.

[41] Liu, L.L.; He, G.Q.; Wang, Y.H.; Liu, P.J. Factors Affecting the Measurement of the Percentage of Gaseous Products from Boron-based Fuel-rich Propellants. *Cent. Eur. J. Energ. Mater.* **2014**, *11*(1): 15-29.

[42] Luo, X.L.; Wang, M.J.; Yun, L.; Yang, J.; Chen, Y.S. Structure-dependent Activities of Cu_2O Cubes in Thermal Decomposition of Ammonium Perchlorate. *J. Phys. Chem. Solids* **2016**, *90*: 1-6.

[43] Rosser, W.A.; Inami, S.H. Thermal Decomposition of Ammonium Perchlorate. *Combust. Flame* **1968**, *12*(5): 427-435.

[44] Lin, X.L.; Zhao, D.M.; Bi, F.Q.; Fan, X.Z.; Zhao, F.Q.; Zhang, G.F.; Zhang, W.Q.; Gao, Z.W. Synthesis, Characterization, Migration Studies and Combustion Catalytic Performances of Energetic Ionic Binuclear Ferrocene Compounds. *J. Organomet. Chem.* **2014**, *762*: 1-8.